Regulation of the Expression of Plant *Resistance* Gene *SNC1* by a Protein with a Conserved BAT2 Domain[1][C][W][OA]

Yingzhong Li, Mark J. Tessaro, Xin Li, and Yuelin Zhang*

College of Life Sciences, Peking University, Beijing 100871, People's Republic of China (Y.L.); National Institute of Biological Sciences, Zhongguancun Life Science Park, Beijing 102206, People's Republic of China (Y.L., Y.Z.); and Michael Smith Laboratories (M.J.T., X.L.) and Department of Botany (X.L.), University of British Columbia, Vancouver, British Columbia, Canada V6T 1Z4

Plant *Resistance* (*R*) genes encode immune receptors that recognize pathogens and activate defense responses. Because of fitness costs associated with maintaining R protein-mediated resistance, expression levels of *R* genes have to be tightly regulated. However, mechanisms on how *R*-gene expression is regulated are poorly understood. Here we show that *MODIFIER OF snc1, 1* (*MOS1*) regulates the expression of *SUPPRESSOR OF npr1-1, CONSTITUTIVE1* (*SNC1*), which encodes a Toll/interleukin receptor-nucleotide binding site-leucine-rich repeat type of R protein in Arabidopsis (*Arabidopsis thaliana*). In the *mos1* loss-of-function mutant plants, *snc1* expression is repressed and constitutive resistance responses mediated by *snc1* are lost. The repression of *snc1* expression in *mos1* is released by knocking out *DECREASE IN DNA METHYLATION1*. In *mos1* mutants, DNA methylation in a region upstream of *SNC1* is altered. Furthermore, expression of *snc1* transgenes using the native promoter does not require *MOS1*, indicating that regulation of *SNC1* expression by *MOS1* is at the chromatin level. Map-based cloning of *MOS1* revealed that it encodes a novel protein with a HLA-B ASSOCIATED TRANSCRIPT2 (BAT2) domain that is conserved in plants and animals. Our study on MOS1 suggests that BAT2 domain-containing proteins may function in regulation of gene expression at chromatin level.

Plant *Resistance* (*R*) genes encode immune receptors that directly or indirectly recognize pathogen effectors (Jones and Dangl, 2006). The largest class of predicted intracellular plant immune receptors is the nucleotide binding site-Leu-rich repeat (NB-LRR) type of R proteins (Meyers et al., 2003), which share structural similarity with mammalian innate immunity receptor NOD proteins. Activation of R proteins often results in quick and robust defense responses including the accumulation of salicylic acid (SA), induction of *PATHOGENESIS-RELATED* (*PR*) gene expression, and localized programmed cell death known as hypersensitive response (Hammond-Kosack and Jones, 1997). Most NB-LRR R proteins contain either a Toll/interleukin receptor (TIR) domain or a coiled-coil domain at the N terminus that probably functions in downstream defense signaling. Interestingly, overexpression of the TIR domain by itself is sufficient to activate cell death (Swiderski et al., 2009).

Arabidopsis (*Arabidopsis thaliana*) *SUPPRESSOR OF npr1-1, CONSTITUTIVE1* (*SNC1*) encodes a TIR-NB-LRR type of R protein (Zhang et al., 2003a). The gain-of-function mutation *snc1* leads to constitutive activation of the R protein and downstream defense responses without the presence of pathogens. *snc1* mutant plants accumulate high levels of SA, constitutively express *PR* genes, and display enhanced resistance to pathogens (Li et al., 2001). An epiallele of *SNC1* known as *bal* also exhibits similar phenotypes as *snc1* (Stokes et al., 2002). Whereas the phenotypes in *snc1* are caused by the deregulated activation of the R protein, the phenotypes of *bal* are caused by increased expression of *SNC1* in the mutant. *bal* was recovered from plants carrying the *decrease in DNA methylation1* (*ddm1*) loss-of-function mutation, which results in a reduction in cytosine methylation throughout the genome (Vongs et al., 1993). But no specific methylation change has been found to correlate with the increased expression of *SNC1* in *bal*. Recently it was shown that the overexpression of *SNC1* in *bal* plants is caused by a 55-kb duplication within the SNC1 locus (Yi and Richards, 2009).

A field test comparing isogenic lines that differ in the presence or absence of *RPM1*, an *R* gene conferring gene-for-gene resistance against the bacterial pathogen *Pseudomonas syringae* carrying the avirulence gene

[1] This work was supported by fundings from the Chinese Ministry of Science and Technology (to Y.Z.) and the Natural Sciences and Engineering Research Council of Canada (to X.L.).

* Corresponding author; e-mail zhangyuelin@nibs.ac.cn.

The author responsible for distribution of materials integral to the findings presented in this article in accordance with the policy described in the Instructions for Authors (www.plantphysiol.org) is: Yuelin Zhang (zhangyuelin@nibs.ac.cn).

[C] Some figures in this article are displayed in color online but in black and white in the print edition.

[W] The online version of this article contains Web-only data.

[OA] Open Access articles can be viewed online without a subscription.

www.plantphysiol.org/cgi/doi/10.1104/pp.110.156240

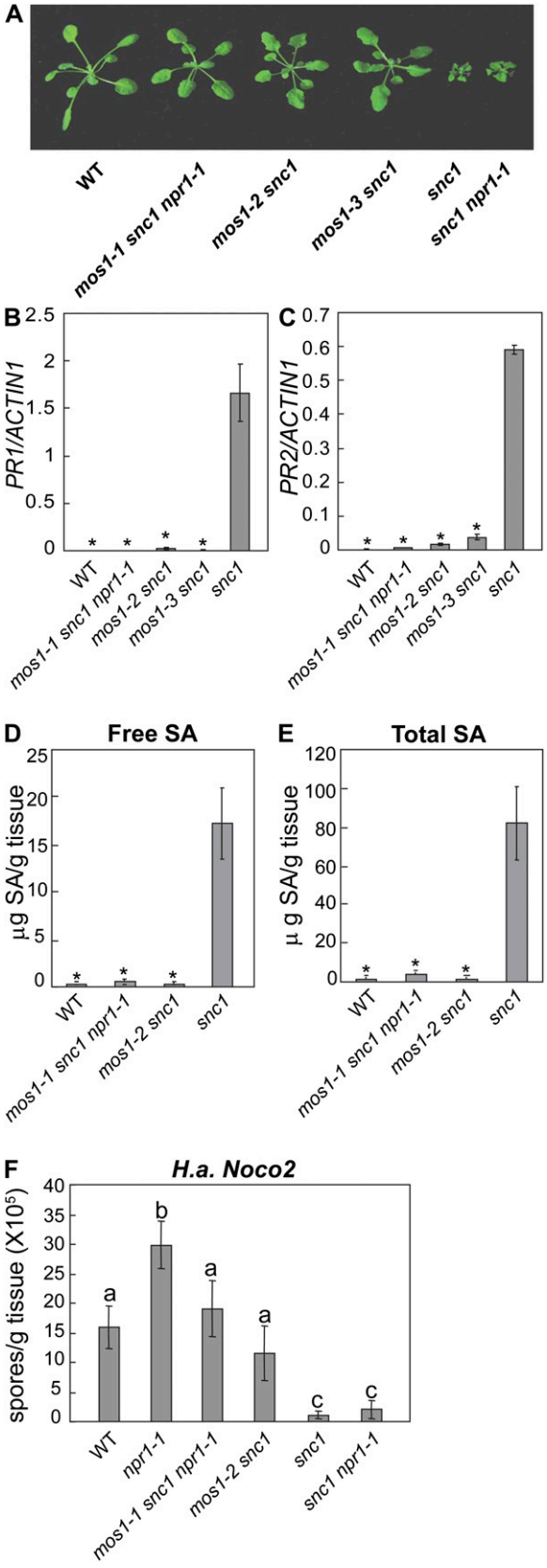

Figure 1. Suppression of *snc1* phenotypes by *mos1* mutants. A, Morphology of 5-week-old soil-grown plants of wild type (WT), *mos1-1 snc1 npr1-1*, *mos1-2 snc1*, *mos1-3 snc1*, *snc1*, and *snc1 npr1-1*. B and C, *PR* gene expression in wild type, *mos1-1 snc1 npr1-1*, *mos1-2 snc1*, *mos1-3 snc1*, and *snc1* seedlings. Total RNA was extracted from 12-d-old seedlings grown on Murashige and Skoog media. Relative expression levels of *PR1* (B) or *PR2* (C) were determined by real-time PCR. Values were normalized to the expression of *ACTIN1*. Error bars represent SD from three measurements. The gene expression analysis was performed on three batches of independent grown plants. Similar results were obtained from different batches of plants and data shown are representatives from one of the experiments. *, $P < 0.001$, significant difference from *snc1*. D and E, SA levels in wild type, *mos1-1 snc1 npr1-1*, *mos1-2 snc1*, and *snc1* plants. SA was extracted from 4-week-old soil-grown plants. Error bars represent SD from four measurements. *, $P < 0.001$, significant difference from *snc1*. F, Growth of *H. arabidopsidis* Noco2 on wild type, *npr1-1*, *mos1-1 snc1 npr1-1*, *mos1-2 snc1*, *snc1*, and *snc1 npr1-1* plants. Two-week-old seedlings were sprayed with *H. arabidopsidis* Noco2 spores (5×10^4 spores/mL). Infection was scored 7 d after inoculation by counting the number of conidia spores. Error bars represent SDs from averages of three measurements. Statistical differences among the samples are labeled with different letters ($P < 0.01$). [See online article for color version of this figure.]

AvrRpm1 or *AvrB*, showed that *RPM1*$^+$ plants had reduced seed production and shoot biomass, suggesting that there is a fitness cost associated with maintenance of *R* gene loci in plants (Tian et al., 2003). In addition, overexpression of *R* genes *Prf1* and *SNC1* leads to constitutive activation of defense responses (Oldroyd and Staskawicz, 1998; Stokes et al., 2002), which is detrimental to plant growth. On the other hand, underexpression of *R* genes can result in loss of R protein function. For example, mutations in *EDM2* lead to reduced expression of the resistance gene *RPP7* and loss of *RPP7*-mediated resistance to *Hyaloperonospora arabidopsidis* isolate Hiks1 (Eulgem et al., 2007). EDM2 belongs to a plant-specific protein family with typical features of transcriptional regulators.

In rice (*Oryza sativa*), expression of the *R* gene *Xa3* is regulated by both genetic backgrounds and developmental stages and expression levels of *Xa3* correlate with the levels of resistance to *Xanthomonas oryzae* pv oryzae (Cao et al., 2007). Moreover, *avrXa27* activates resistance responses through induction of the expression of its cognate *R* gene *Xa27* (Gu et al., 2005). Thus, controlling the expression levels of *R* genes plays important roles in the regulation of plant defense responses. In a *snc1* suppressor screen that identified multiple *mos* mutants affecting signal transduction downstream of *snc1* (Zhang and Li, 2005), we also found multiple alleles of *modifier of snc1, 1* (*mos1*) that inactivate *snc1* through repression of the *SNC1* locus, suggesting that MOS1 plays an important role in maintaining the expression of *SNC1*.

RESULTS

Identification and Characterization of *mos1* Mutant Alleles

Arabidopsis *npr1* is required for SA-induced *PR* gene expression (Dong, 2004). In *snc1 npr1-1* mutant

plants, *PR* gene expression and pathogen resistance are constitutively activated (Li et al., 2001). A classical suppressor screen was carried out to identify genes required for activation of defense responses in the *snc1* or *snc1 npr1* mutant using fast neutron-mutagenized populations (Zhang and Li, 2005). Multiple genes have been reported to be required for *snc1*-mediated resistance (Zhang et al., 2005; Palma et al., 2005; Zhang and Li, 2005; Goritschnig et al., 2007; Palma et al., 2007; Goritschnig et al., 2008; Monaghan et al., 2009). From the same mutant screen, two alleles of *mos1* (*mos1-1* and *mos1-2*) were also identified. A third allele of *mos1*, *mos1-3*, was recovered from a T-DNA mutant population in the *snc1* background. The *mos1-1 snc1 npr1-1*, *mos1-2 snc1*, and *mos1-3 snc1* plants are similar to wild-type Columbia-0 (Col-0) plants in size (Fig. 1A). Backcrossing of *mos1-1 snc1 npr1-1* and *mos1-2 snc1* to *snc1* showed that all F1 plants were *snc1* like, indicating that *mos1-1* and *mos1-2* are both recessive mutations.

In *snc1* mutant plants, *PR* gene expression is constitutively activated. As shown in Figure 1, B and C, the expression of *PR1* and *PR2* in *snc1* is suppressed by the *mos1* mutations. In *snc1* mutant plants, SA also accumulates to high levels (Li et al., 2001). To determine whether *mos1-1* and *mos1-2* affects the SA level in *snc1*, total SA and free SA in *mos1-1 snc1 npr1* and *mos1-2 snc1* plants were extracted and quantified. As shown in Figure 1, D and E, both free SA and total SA in *snc1* are dramatically reduced by the *mos1-1* and *mos1-2* mutations.

To test whether constitutive pathogen resistance in *snc1* is affected by the *mos1* mutations, *mos1-1 snc1 npr1* and *mos1-2 snc1* plants were inoculated with the virulent oomycete pathogen *H. arabidopsidis* Noco2. While *snc1* and *snc1 npr1* plants were resistant to the pathogen, the *mos1-1 snc1 npr1* and *mos1-2 snc1* plants completely lost the enhanced resistance in *snc1* (Fig. 1F).

MOS1 Encodes a Protein with a HLA-B ASSOCIATED TRANSCRIPT2 Domain That Is Conserved in Plants and Animals

To map the *mos1-1* mutation, *mos1-1 snc1* (in the Col-0 ecotype background) was crossed with Landsberg *erecta* (L*er*) in which the *snc1* locus has been introgressed to generate a segregating F2 population. Crude mapping showed that *mos1-1* is located south of *snc1* on chromosome 4. Unfortunately the region where *mos1-1* is located is derived from the Col-0 ecotype in the L*er-snc1* line. Thus, for fine mapping, *mos1-1 snc1* was crossed with L*er*. Plants with *snc1*-like morphology were selected from the F2 population. These plants should be homozygous for the *snc1* mutation and heterozygous for the *mos1-1* mutation due to recombination. About 800 F3 plants derived from the F2 lines that were homozygous for *snc1* and heterozygous for *mos1-1* were genotyped with the markers T13J8 and F16G20. The *mos1-1* mutation was further mapped to a 110-kb region between marker

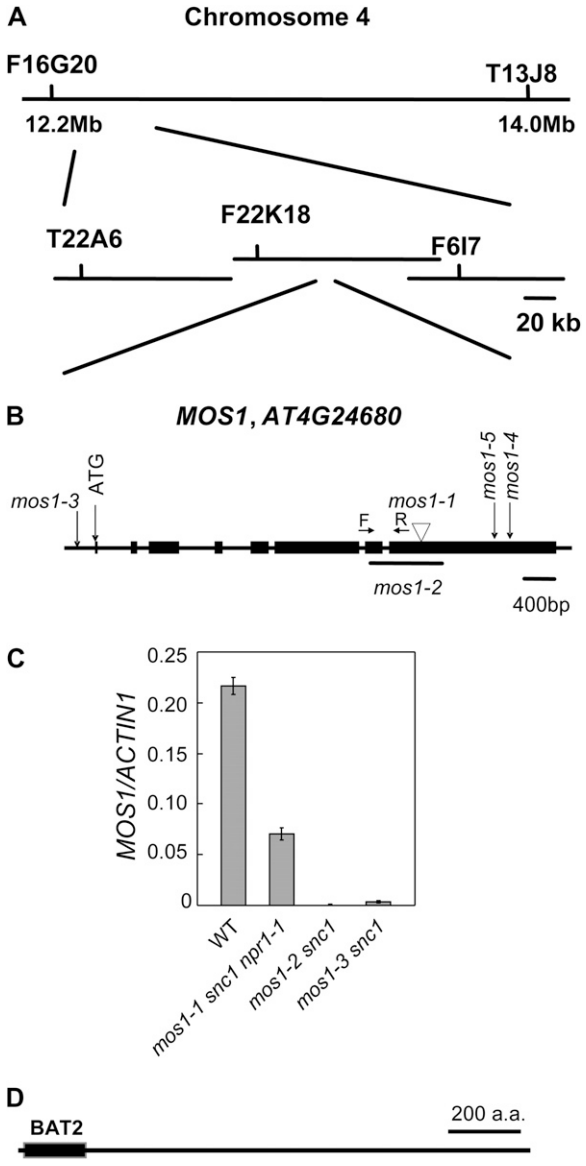

Figure 2. Map-based cloning of *mos1*. A, Map position of *mos1-1* on chromosome 4. BAC clones and markers are indicated. B, Gene structure of *MOS1* (*At4g24680*). Exons are indicated by boxes. Introns and untranslated regions are represented by solid lines. The locations of *mos1-1* and *mos1-2* deletions and the T-DNA insertion in *mos1-3*, *mos1-4* (salk_126709), and *mos1-5* (salk_074876) are indicated. The positions of the T-DNA were confirmed by PCR. C, *MOS1* expression in wild type, *mos1-1 snc1 npr1-1*, *mos1-2 snc1*, and *mos1-3 snc1* plants. Total RNA was extracted from 2-week-old seedlings grown on Murashige and Skoog medium. Relative expression level of *MOS1* was determined by real-time PCR. The positions of the primers (forward [F] and reverse [R]) are shown in B. Values were normalized to the expression of *ACTIN1*. Error bars represent SD from three measurements. The gene expression analysis was performed on three batches of independent grown plants. Similar results were obtained from different batches of plants and data shown are representatives from one of the experiments. D, Protein structure of MOS1. a.a., Amino acids; WT, wild type.

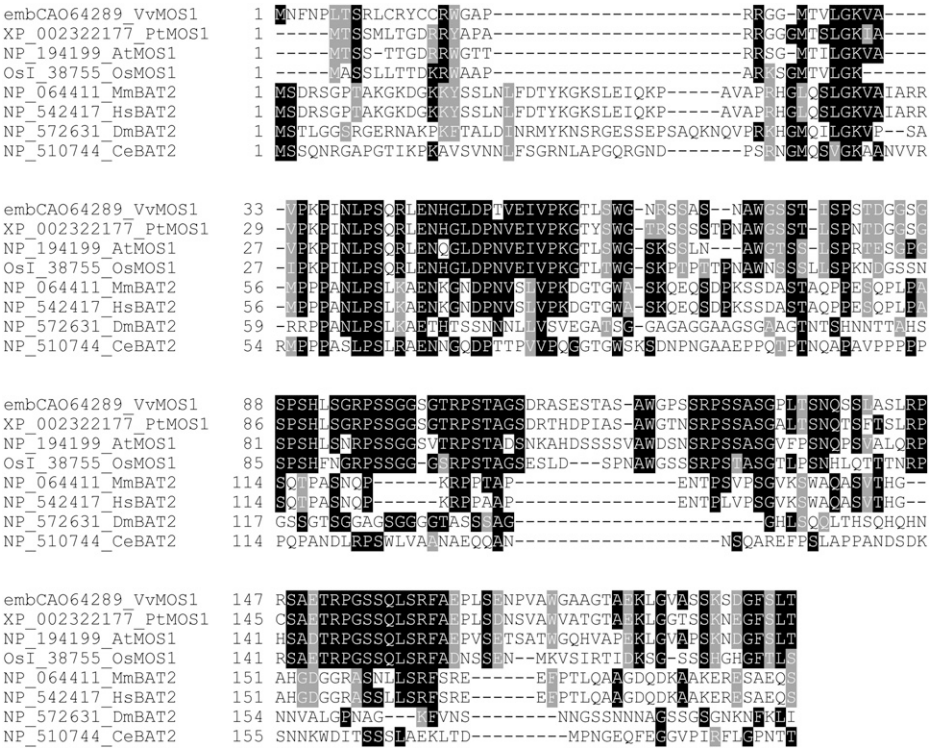

Figure 3. Alignment of BAT2 domains of proteins from different eukaryotic species. The BAT2 domains from Arabidopsis MOS1 (AtMOS1), rice MOS1 (OsI_38755_OsMOS1), grapevine (*Vitus vinifera*) MOS1 (embCAO64289_VvMOS1), poplar (*Populus trichocarpa*) MOS1 (XP_002322177_PtMOS1), human BAT2 (NP_542417_HsBAT2), mouse BAT2 (NP_064411_MmBAT2), and two BAT2-domain-containing protein from *Drosophila melanogaster* (DmBAT2) and *C. elegans* (CeBAT2) were aligned with ClustalX 2.0.11 and shaded with BOXSHADE (http://www.ch.embnet.org/software/BOX_form.html).

F22K18 and F6I7 after analyzing recombinants between T13J8 and F16G20 (Fig. 2A).

To search for the molecular lesion in *mos1-1*, the region between F22K18 and F6I7 in *mos1-1 snc1* was amplified by PCR and sequenced. Comparison with the Col-0 sequence showed that *mos1-1* contains an 8-bp deletion in the coding region of *AT4G24680* (Fig. 2B). PCR analysis on *mos1-2 snc1* revealed that the 3′ half of *At4g24680* was deleted in *mos1-2 snc1*. Expression of *MOS1* in *mos1-2* was dramatically reduced (Fig. 2C). The third allele of *mos1*, *mos1-3*, was isolated after we cloned the *MOS1* gene. Inverse PCR showed that

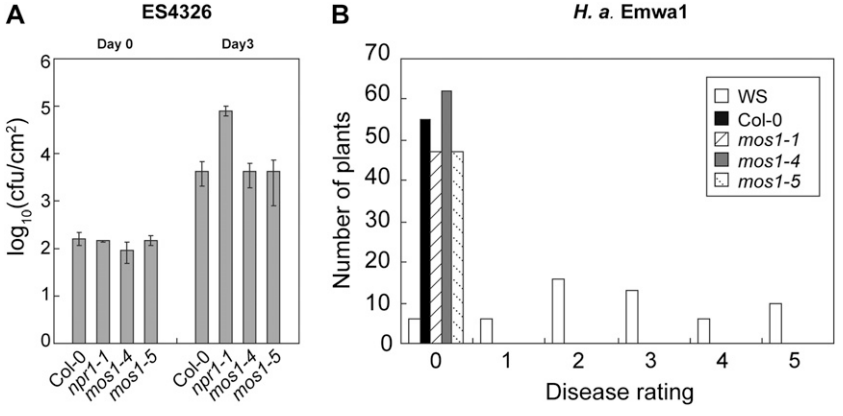

Figure 4. Analysis of pathogen resistance in *mos1* single-mutant plants. A, Growth of *P. syringae* pv *maculicola* ES4326 in Col-0, *npr1-1*, *mos1-4*, and *mos1-5* plants. The leaves of 4-week-old soil-grown plants were infiltrated with a suspension of the bacteria at OD600 = 0.0001. Leaf discs within the inoculated areas were taken 3 d after inoculation. Error bars represent SD from measurements of four independent samples. Each sample contained two leaf discs from two different infiltrated leaves on the same plant. cfu, Colony-forming units. B, Growth of *H. arabidopsidis* Emwa1 on Wassilewskija (WS), Col-0, *mos1-1*, *mos1-4*, and *mos1-5* plants. Two-week-old seedlings were sprayed with Emwa1 spores at a conidiospore suspension concentration of 50,000 spores per mL of water. The infection was rated as follows on 20 plants 7 d after infection by counting the number of conidiophores per infected leaf: 0, no conidiophores on the plants; 1, no more than five conidiophores per infected leaf; 2, six to 20 conidiophores on a few of the infected leaves; 3, six to 20 conidiophores on most of the infected leaves; 4, five or more conidiophores on all infected leaves; 5, 20 or more conidiophores on all infected leaves.

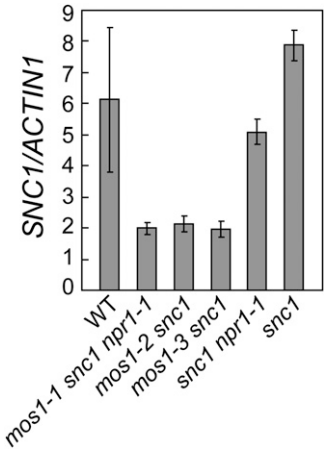

Figure 5. *mos1* mutations suppress *snc1* expression. *SNC1/snc1* expression in wild type (WT), *mos1-1 snc1 npr1-1*, *mos1-2 snc1*, *mos1-3 snc1*, *snc1 npr1-1*, and *snc1*. Total RNA was extracted from 12-d-old seedlings grown on Murashige and Skoog medium. Relative expression levels of *snc1* were determined by real-time PCR. Values were normalized to the expression of *ACTIN1*. Error bars represent SD from three measurements. The gene expression analysis was performed on three batches of independent grown plants. Similar results were obtained from different batches of plants and data shown are representatives from one of the experiments.

mos1-3 contains a T-DNA insertion in the promoter region of *MOS1*, which abolished *MOS1* expression in *mos1-3* (Fig. 2C). Two T-DNA alleles of *mos1*, *mos1-4*, and *mos1-5*, were also found in the Salk T-DNA collection. Reverse transcription (RT)-PCR analysis showed that the expression of *MOS1* was blocked in *mos1-4* and *mos1-5* (Supplemental Fig. S1), indicating they are loss-of-function alleles.

Analysis of the cDNA sequence of *MOS1* revealed that it encodes a large protein with 1,412 amino acids. The N terminus of MOS1 contains a conserved HLA-B ASSOCIATED TRANSCRIPT2 (BAT2) domain (Fig. 2D). BLAST search of the GenBank showed the N-terminal domain of MOS1 is similar to the mouse BAT2 protein with an *E* value of 8×10^{-5}. The rest of the protein is rich in hydrophilic residues. A nuclear localization signal (PKKGNKR, amino acid 1,192–1,198) was found at the C terminus of MOS1. Proteins with BAT2 domains are present in most multicellular organisms, most of which contain the BAT2 domain at the N terminus and a large region with mainly hydrophilic residues at the C terminus. The function of the BAT2 domain is unknown. Alignment of the BAT2 domains from various proteins containing this domain is shown in Figure 3.

To detect MOS1 protein, we generated a MOS1-specific antibody in rabbit using a fragment of MOS1 containing the N-terminal 235 amino acid. The antibody was capable of detecting 0.006 ng of recombinant protein expressed in *Escherichia coli* (Supplemental Fig. S2). The steady-state protein levels of MOS1 in plants appear to be very low, as we were not able to detect the protein using this antibody. In addition, we were not able to detect the MOS1 protein in transgenic plants expressing MOS1-GFP or MOS1-3xFLAG fusion protein under either its native promoter or the constitutive 35S promoter using commercial anti-GFP and anti-FLAG antibodies, suggesting that the level of MOS1 is extremely low in Arabidopsis. Analysis of *MOS1* expression using the microarray database at The Arabidopsis Information Resource found no obvious induction of its expression under various biotic and abiotic treatments.

MOS1 Regulates *SNC1* Expression Levels at Chromatin Level

Since *mos1* was one of the most complete suppressors of *snc1*, we first hypothesized that MOS1 may function in defense signal transduction. However, we found that *mos1* single mutants exhibit no defects in basal resistance against the bacterial pathogen *P. syringae* pv *maculicola* ES4326 (Fig. 4A). In addition, resistance to *H. arabidopsidis* Emwa1 mediated by RPP4, an R protein closely related to SNC1, is not affected by the *mos1* mutations (Fig. 4B), suggesting that MOS1 may not be a general signaling regulator functioning downstream of *snc1*.

We then tested whether *mos1* mutations affect the expression of *snc1* by comparing the expression levels of *snc1* in *mos1-1 snc1 npr1-1*, *mos1-2 snc1*, *mos1-3 snc1*, *snc1*, *snc1 npr1*, and wild-type plants. As shown in Figure 5, *snc1* expression is reduced about 3-fold in *mos1-1 snc1 npr1-1*, *mos1-2 snc1*, and *mos1-3snc1* mutant plants compared to that in wild type, suggesting that *MOS1* is required for maintaining proper expression levels of *snc1*. Reduction of *SNC1* expression was also observed in the *mos1* single mutants (Supplemental Fig. S3).

To determine whether *mos1* mutations affect *SNC1* expression in a locus-specific manner, we transformed a genomic clone (*pSNC1*::*snc1*) expressing the *snc1* mutant gene under its own promoter into wild-type and *mos1-2 snc1* plants (Zhang et al., 2003a). The size of the promoter fragment used is 1.8 kb. As shown in Table I, about 70% of transgenic plants in the wild-type background exhibited *snc1*-like morphology. A similar percentage of transgenic plants was found to display *snc1*-like morphology in the *mos1-2 snc1* background (Fig. 6A). Similar results were obtained when *snc1* was expressed under a 2.5-kb promoter fragment. These data suggest that *mos1-2* is not able to suppress the expression of the *snc1* transgene inserted elsewhere in the genome.

Table I. *Percentage of transgenic plants expressing the snc1 transgene that exhibited snc1-like morphology*

Summary of T1 Transgenic plants.

Transgenic Type	Wild-Type Like	*snc1* Like	Total
snc1 in wild type	37 (37.8%)	61 (62.2%)	98
snc1 in *mos1-2 snc1*	20 (37.0%)	34 (63.0%)	54

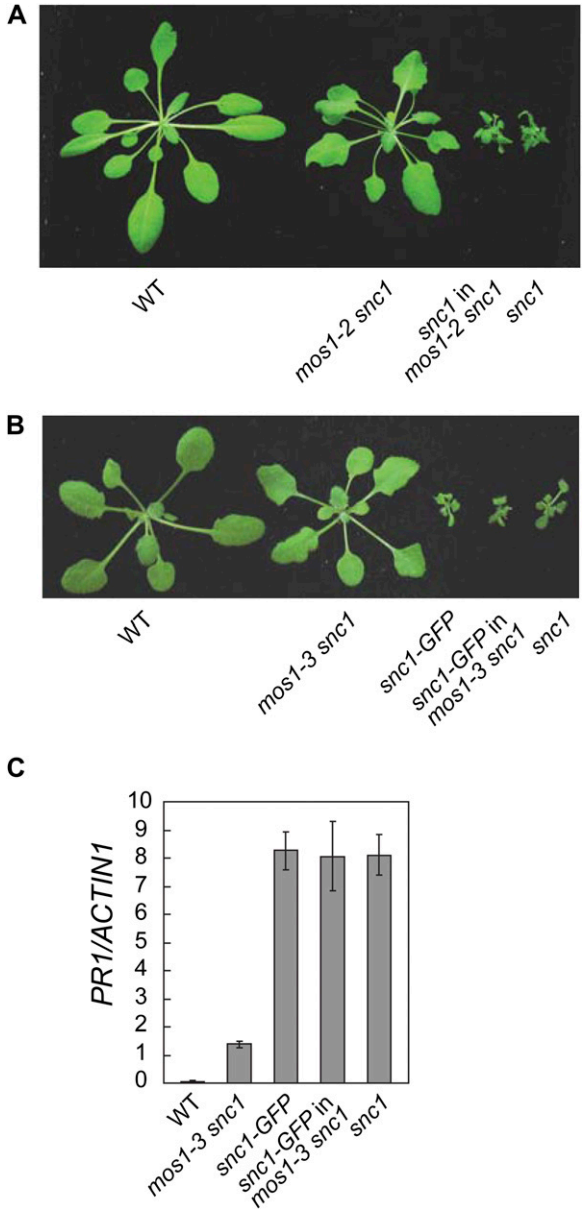

Figure 6. Suppression of *snc1* expression by *mos1* is locus specific. A, Morphology of 5-week-old soil-grown plants of wild type (WT), *mos1-2 snc1*, a representative line of *mos1-2 snc1* transformed with the *snc1* genomic clone, and *snc1*. B, Morphology of 5-week-old soil-grown plants of wild type, *mos1-3 snc1*, the *snc1*::*GFP* line, *mos1-3 snc1* with the *snc1*::*GFP* transgene, and *snc1*. C, *PR1* expression in the indicated genotypes. Total RNA was extracted from 12-d-old seedlings grown on Murashige and Skoog medium. Relative expression levels of *PR1* were determined by real-time PCR. Values were normalized to the expression of *ACTIN1*. Error bars represent SD from three measurements. The gene expression analysis was performed on three batches of independent grown plants. Similar results were obtained from different batches of plants and data shown are representatives from one of the experiments. [See online article for color version of this figure.]

To further confirm that expression of *snc1* in transgenic plants does not require *MOS1*, we crossed the *mos1-3* mutation into a transgenic line expressing the mutant snc1-GFP fusion protein under its own promoter. The expression level of the *snc1-GFP* transgene is comparable to that of the endogenous wild-type *SNC1* (Supplemental Fig. S4). As shown in Figure 6B, the *snc1*-like morphology in the transgenic plants is not affected by the *mos1-3* mutation. In addition, the expression levels of *PR1* in the transgenic line are not altered by the *mos1-3* (Fig. 6C). These data suggest that *MOS1* regulates the expression of *snc1* in a locus-specific manner, probably at the chromatin level.

ddm1 Releases the Repression of *snc1* Expression in *mos1-1 snc1 npr1* Plants

Arabidopsis *ddm1* was originally identified in a screen for mutants with decreased cytosine methylation (Vongs et al., 1993). *ddm1* mutations lead to reduced 5-methylcytosine levels throughout the genome. *DDM1* encodes a SWI2/SNF2-like protein that most likely functions in chromatin remodeling (Jeddeloh et al., 1999) and it is required for maintenance of gene silencing in Arabidopsis (Jeddeloh et al., 1998). To test whether silencing of the *snc1* locus caused by the loss of *MOS1* function requires *DDM1*, we crossed *mos1-1 snc1 npr1-1* with *ddm1-8* (SALK_093009), an allele of *ddm1* that contains a T-DNA insertion at the 3′ end of DDM1 (Supplemental Fig. S5A). RT-PCR analysis showed that the full-length cDNA of *DDM1* was no longer expressed in the mutant (Supplemental Fig. S5B). Like other *ddm1* alleles, *ddm1-8* causes hypomethylation of the 180-bp centromere repeats in addition to the 5SRNA locus (Supplemental Fig. S5, C and D).

As shown in Figure 7A, *ddm1-8* reverted *mos1-1 snc1 npr1-1* back to *snc1*-like morphology. The *snc1*-like morphology was not caused by duplication of the *snc1* locus like that in *bal* since no duplication of the locus was found in *ddm1-8 mos1-1 snc1* (Supplemental Fig. S6). Constitutive expression of *PR1* and *PR2* and resistance to *H. arabidopsidis* Noco2 were also restored in *ddm1-8 mos1-1 snc1* (Fig. 7, B–D). Real-time RT-PCR analysis showed that *snc1* expression in *ddm1-8 mos1-1 snc1* is reverted to the level in wild type (Fig. 7E), suggesting that *ddm1* releases the silencing of the *snc1* locus in *mos1-1 snc1 npr1-1*. These results indicate that MOS1 may be involved in regulating chromatin structure at the *snc1* locus antagonistic to DDM1.

mos1 Alters Methylation of DNA Upstream of *SNC1*

As DDM1 functions as a putative chromatin remodeling factor and loss of DDM1 function results in reduced DNA methylation, alteration of chromatin structure may cause changes in DNA methylation. To determine whether methylation of DNA upstream of *SNC1* is altered in *mos1* mutant plants, bisulfite conversion sequencing was performed on the regions upstream of *SNC1*. We only detected DNA methylation in a region about 3 kb away from the coding region of *SNC1* (Supplemental Fig. S7). The methylation levels in various genotypes are shown in Figure 8.

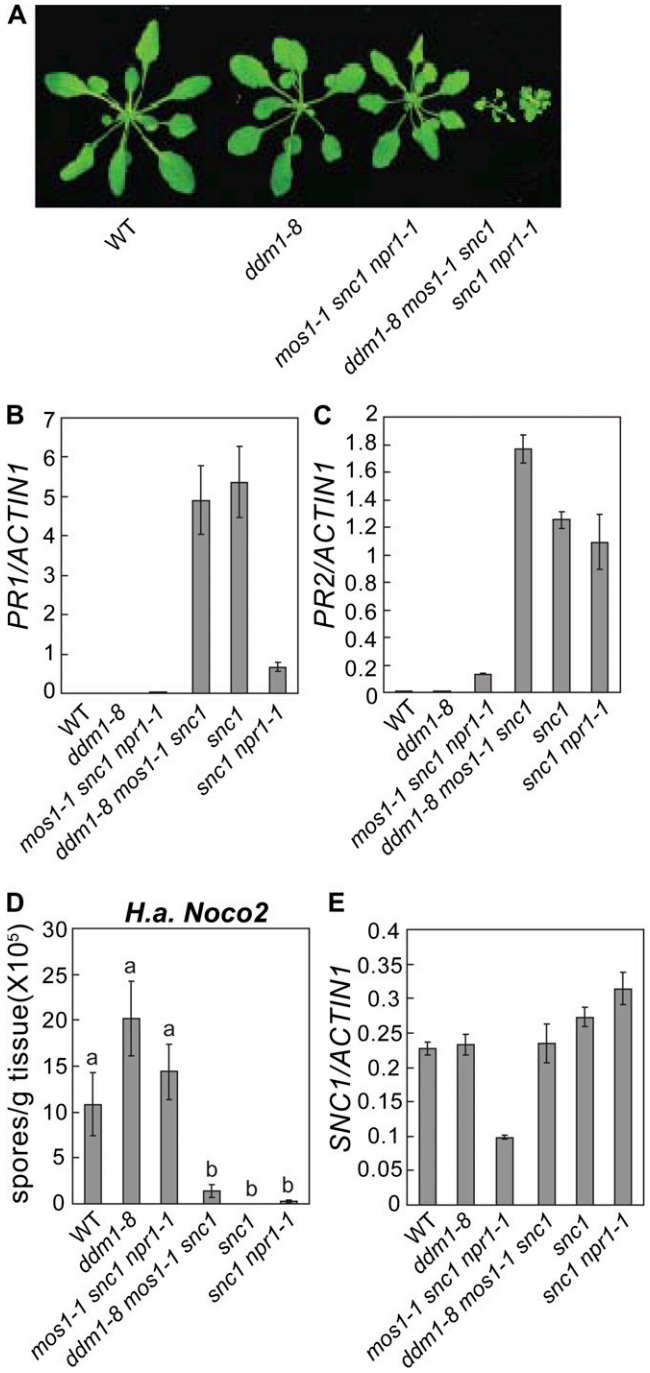

Figure 7. *ddm1* releases the repression of *snc1* expression by *mos1-1*. A, Morphology of 5-week-old soil-grown plants of wild type (WT), *ddm1-8*, *mos1-1 snc1 npr1-1*, *ddm1-8 mos1-1 snc1*, and *snc1 npr1-1*. B and C, *PR* gene expression in wild type, *ddm1-8*, *mos1-1 snc1 npr1-1*, *ddm1-8 mos1-1 snc1*, *snc1*, and *snc1 npr1-1*. Total RNA was extracted from 12-d-old seedlings grown on Murashige and Skoog medium. Relative expression levels of *PR1* (B) or *PR2* (C) were determined by real-time PCR. Values were normalized to the expression of *ACTIN1*. Error bars represent SD from three measurements. D, Growth of *H. arabidopsidis* Noco2 on wild type, *ddm1-8, mos1-1 snc1 npr1-1*, *ddm1-8 mos1-1 snc1*, *snc1*, and *snc1 npr1-1* plants. Twelve-day-old seedlings were sprayed with *H. arabidopsidis* Noco2 (5×10^4 spores/mL). Infection was scored 7 d post inoculation by counting the number of conidia spores. Error bars represent SDs from averages of three measurements. Statistical differences among the samples are labeled with different letters ($P < 0.01$). E, *SNC1*/*snc1* expression in wild type, *ddm1-8*, *mos1-1 snc1 npr1-1*, *ddm1-8 mos1-1 snc1*, *snc1*, and *snc1 npr1-1* plants. Total RNA was extracted from 12-d-old seedlings grown on Murashige and Skoog medium. Relative expression levels of *SNC1*/*snc1* were determined by real-time PCR. Values were normalized to the expression of *ACTIN1*. Error bars represent SD from three measurements. All gene expression analysis was performed on three batches of independent grown plants. Similar results were obtained from different batches of plants and data shown are representatives from one of the experiments. [See online article for color version of this figure.]

mCG level decreased dramatically in the first three CG sites in *snc1*, compared to that in wild-type plants. The *mos1-1* mutation has no obvious effect on CG methylation at these sites (Fig. 8A). Interestingly, methylation levels at two of the eight CNG sites are clearly increased in *snc1* plants and reduced in *mos1-1 snc1 npr1* and *mos1-1 snc1* mutants (Fig. 8B). The difference in methylation at the CHH sites is even more dramatic. As shown in Figure 8C, methylation levels at seven of the 10 CHH sites are increased in *snc1* plants and reduced close to wild-type levels in *mos1-1 snc1 npr1* and *mos1-1 snc1* mutants. These data further support that MOS1 is involved in the regulation of the chromatin structure and DNA methylation at the *SNC1* locus.

DISCUSSION

Here we report that MOS1 regulates *snc1*-mediated resistance responses by fine-tuning *SNC1* expression. Several lines of evidence suggest that MOS1 regulates the SNC1 locus at chromatin level. First, *mos1* mutations reduce the expression of endogenous *snc1* but not the *snc1* transgene under its own promoter, indicating that MOS1 regulates the expression of *snc1* in a locus-specific manner. Second, suppression of *snc1* expression in the *mos1* mutant plants can be reversed by knocking out the known epigenetic regulator DDM1, which functions in chromatin remodeling and DNA methylation (Vongs et al., 1993). Finally, *mos1* mutations result in alterations of DNA methylation in a region upstream of *SNC1*.

MOS1 encodes a large protein with a BAT2 domain at its N terminus. BAT2 domains are found in large proteins with similar features from many plant and animal species. The BAT2 domain is found at the N terminus, and the rest of the protein consists of mainly hydrophilic residues. None of these proteins have previously been functionally characterized. Our studies on MOS1 suggest that this family of proteins may function in regulating gene expression at the chromatin level. In the *mos1* mutants, the expression of *RPP4*, a resistance gene next to *SNC1*, was also modestly reduced (Supplemental Fig. S8). This is consistent with the previous report that genes in the *RPP4* cluster are coordinately regulated at the transcription level

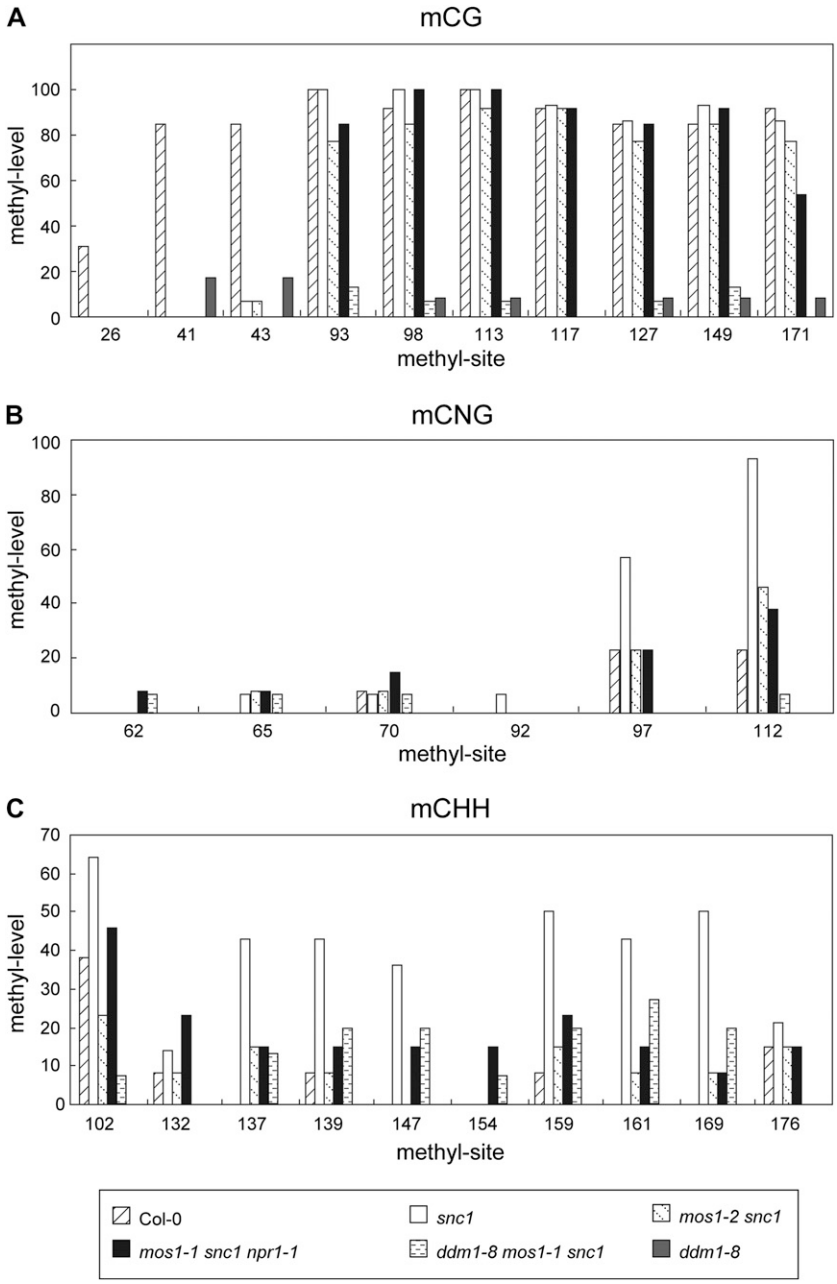

Figure 8. DNA methylation levels of a region upstream of *SNC1*. Bisulfite conversion sequencing results of mCG (A), mCNG (B), and mCHH (C) in wild type, *snc1*, *mos1-2 snc1*, *mos1-1 snc1 npr1-1*, *ddm1-8 mos1-1 snc1*, and *ddm1-8* mutant plants. The sequenced region is about 3 kb upstream of the ATG of *SNC1*. N represents any base. H represents any base except for G. The unconverted original sequence and the position of different methyl sites are shown in Supplemental Figure S7.

(Yi and Richards, 2007). In addition to loss of *snc1*-mediated immune responses, the *mos1* mutant plants also displayed late-flowering phenotype (Supplemental Fig. S9), suggesting that MOS1 also regulates gene expression at other loci.

In the *mos1* mutants, alteration of DNA methylation was observed in a region upstream of *SNC1*. Because no obvious correlation was found between the observed methylation changes and the reduced expression levels of *snc1*, reduction of *snc1* expression was not caused by these methylation changes. Since BAT2 domain-containing proteins similar to MOS1 are present in a wide range of eukaryotes including species with no DNA methylation such as *Caenorhabditis elegans*, MOS1 may not function on DNA methylation directly. Rather, MOS1 probably functions as a regulator of chromatin structure, and the silencing of *SNC1* in *mos1* mutants is probably caused by changes in the chromatin structure around the *SNC1* locus. The alteration of DNA methylation may also be a result of chromatin structure change. Interestingly, we also observed methylation differences in some of the sites between wild type and *snc1*. It is unclear how these changes arose.

In *ddm1* mutant plants, the expression of *SNC1* is comparable to that in the wild-type plants, suggesting that *ddm1* mutations do not directly cause up-regulation of the *SNC1* locus. Interestingly, the suppression of *snc1*

expression in *mos1* mutant plants was reversed by knocking out the function of *DDM1*, suggesting that MOS1 and DDM1 function antagonistically to fine-tune the expression of *SNC1* at the chromatin level. It remains to be determined whether regulation of *R* gene expression at chromatin level is a common phenomenon.

MATERIALS AND METHODS

Mutant Screen and Characterization

All plants were grown under 16 h light at 23°C and 8 h dark at 20°C. *mos1-1 snc1 npr1* was identified from a fast neutron-treated *snc1 npr1* mutant population while *mos1-2 snc1* was identified from a fast neutron-treated *snc1* mutant population as previously described (Zhang et al., 2003a). *mos1-3* was isolated from T2 plants of a T-DNA population consisting of approximately 60,000 independent T1 transgenic lines generated by transforming *snc1* with pSKi015 (Weigel et al., 2000). The T-DNA insertion site in *mos1-3* was identified by inverse PCR.

Seeds of *mos1-4* (salk_126709), *mos1-5* (salk_074876), and *ddm1-8* (salk_093009) were obtained from the Arabidopsis Biological Resource Center. Homozygous plants were identified by PCR using primers flanking the insertion. *ddm1 mos1-1 snc1* triple mutant was generated by crossing *ddm1-8* with *mos1-1 snc1-1 npr1* and genotyping the F2 population. The primers used to identify the *mos1-1* mutation are MOS1-WT (5′-gttattgcttgagacaccttc-3′) and 43950R (5′-aaggcaatgatgcttggcag-3′).

Infection of *Hyaloperonospora arabidopsidis* Noco2 was performed on 2-week-old seedlings by spraying with a *H. arabidopsidis* Noco2 spore suspension at a concentration of 5×10^4 spores per mL of water. The plants were kept at 18°C in 12-h light/12-h dark cycles with 95% humidity, and the infection was scored 7 d after inoculation by counting the number of conidiaspores per gram of leaf tissue using a hemocytometer.

For gene expression analysis, RNA was extracted from 12-d-old seedlings grown on Murashige and Skoog medium at 23°C under 16-h light/8-h dark cycles using Takara RNAiso reagent. RT was carried out using the M-MLV RTase cDNA synthesis kit from Takara. Real-time PCR was performed using the SYBR Premix Ex (Takara). All expression analysis was performed on three batches of independent grown plants. The primers used for amplification of *Actin1*, *PR1*, and *PR2* were described previously (Zhang et al., 2003a, 2003b). The primers for amplification of *SNC1* are SNC1-F (5′-gaatcgaatgtctctatctgc-3′) and SNC1-R (5′-ctgtaaagtcggcgagctca-3′). SA was extracted and measured using a previously described procedure (Li et al., 1999).

Map-Based Cloning of *mos1*

Mapping markers were designed based on the Monsanto Arabidopsis (*Arabidopsis thaliana*) polymorphism and Landsberg sequence collections (Jander et al., 2002). Marker primers used for PCR include T13J8, 5′-ttataagctcccttgtagtga-3′ and 5′-agtaagatctatgtgacttgg-3′; F16G20, 5′-caaaggcatgtacgtagttgca-3′ and 5′-cttatttttggcgtgctagttac-3′; F6I7, 5′-agcacgatcgtaagcactcc-3′ and 5′-agatgactgtcgacttgcca-3′; and F22K18, 5′-tcacggagcaaaagctcgca-3′ and 5′-cataactggaggtggtgttg-3′. Markers T13J8 and F16G20 are based on Indel polymorphisms. The polymorphisms between Col-0 and L*er* for markers F6I7 and F22K18 were detected by restriction digestion of the PCR fragments with *Sal*I and *Mbo*II, respectively.

Bisulfite Sequencing

Genomic DNA was extracted from 30-d-old seedlings using DNeasy plant mini kit (Qiagen catalog no. 69104). Bisulfite treatment of genomic DNA was performed using a DNA modification kit following the manufacturer's instructions (Chemicon catalog no. S7820). The primers (5′-TAAGGATATAGGTTTGAATAATGAT-3′ and 5′-TTACACTAAAAAATAAACCTCATAAATAAT-3′) used to amply DNA fragments after bisulfate treatment were designed using MethPrimer (http://www.urogene.org/methprimer/index1.html). PCR fragments amplified from the bisulfite-treated DNA were cloned into pGEM-T easy vector (Promega).

Sequence data from this article can be found in the GenBank/EMBL data libraries under accession number HM208348.

Supplemental Data

The following materials are available in the online version of this article.

Supplemental Figure S1. Expression of *MOS1* in *mos1-4*, *mos1-5*, and wild-type plants.

Supplemental Figure S2. Western-blot analysis of recombinant MOS1 protein using an anti-MOS1 antibody.

Supplemental Figure S3. *SNC1* expression in Col-0, *mos1-1*, *mos1-4*, and *mos1-5*.

Supplemental Figure S4. *SNC1* expression in Col-0 wild type and the *snc1-GFP* transgenic line in wild-type background.

Supplemental Figure S5. Characterization of *ddm1-8*.

Supplemental Figure S6. Analysis of *snc1* copy numbers in the wild type and *ddm1-8 mos1-1 snc1*.

Supplemental Figure S7. Alignment of the bisulfite converted sequences of a region about 3 kb upstream of *SNC1*.

Supplemental Figure S8. *RPP4* expression in Col-0, *mos1-1*, *mos1-4*, and *mos1-5*.

Supplemental Figure S9. Mutations in *MOS1* lead to a late-flowering phenotype in Arabidopsis.

ACKNOWLEDGMENTS

We thank the Arabidopsis Biological Resource Center for the T-DNA mutant *ddm1-8* and Dr. Eric Richards for plasmids containing the 180-bp centromere repeats and 5S rDNA. We greatly appreciate Ms. Dongling Bi and Ms. Yu Ti Cheng for technical assistance, and Ms. Jacqueline Monaghan for critical reading of the manuscript.

Received March 15, 2010; accepted April 29, 2010; published May 3, 2010.

LITERATURE CITED

Cao Y, Ding X, Cai M, Zhao J, Lin Y, Li X, Xu C, Wang S (2007) The expression pattern of a rice disease resistance gene xa3/xa26 is differentially regulated by the genetic backgrounds and developmental stages that influence its function. Genetics **177:** 523–533

Dong X (2004) NPR1, all things considered. Curr Opin Plant Biol **7:** 547–552

Eulgem T, Tsuchiya T, Wang XJ, Beasley B, Cuzick A, Tor M, Zhu T, McDowell JM, Holub E, Dangl JL (2007) EDM2 is required for RPP7-dependent disease resistance in Arabidopsis and affects RPP7 transcript levels. Plant J **49:** 829–839

Goritschnig S, Weihmann T, Zhang Y, Fobert P, McCourt P, Li X (2008) A novel role for protein farnesylation in plant innate immunity. Plant Physiol **148:** 348–357

Goritschnig S, Zhang Y, Li X (2007) The ubiquitin pathway is required for innate immunity in Arabidopsis. Plant J **49:** 540–551

Gu K, Yang B, Tian D, Wu L, Wang D, Sreekala C, Yang F, Chu Z, Wang GL, White FF, et al (2005) R gene expression induced by a type-III effector triggers disease resistance in rice. Nature **435:** 1122–1125

Hammond-Kosack KE, Jones JD (1997) Plant disease resistance genes. Annu Rev Plant Physiol Plant Mol Biol **48:** 575–607

Jander G, Norris SR, Rounsley SD, Bush DF, Levin IM, Last RL (2002) Arabidopsis map-based cloning in the post-genome era. Plant Physiol **129:** 440–450

Jeddeloh JA, Bender J, Richards EJ (1998) The DNA methylation locus DDM1 is required for maintenance of gene silencing in Arabidopsis. Genes Dev **12:** 1714–1725

Jeddeloh JA, Stokes TL, Richards EJ (1999) Maintenance of genomic methylation requires a SWI2/SNF2-like protein. Nat Genet **22:** 94–97

Jones JD, Dangl JL (2006) The plant immune system. Nature **444:** 323–329

Li X, Clarke JD, Zhang Y, Dong X (2001) Activation of an EDS1-mediated R-gene pathway in the snc1 mutant leads to constitutive, NPR1-independent pathogen resistance. Mol Plant Microbe Interact **14:** 1131–1139

Li X, Zhang Y, Clarke JD, Li Y, Dong X (1999) Identification and cloning of

a negative regulator of systemic acquired resistance, SNI1, through a screen for suppressors of npr1-1. Cell **98:** 329–339

Meyers BC, Kozik A, Griego A, Kuang H, Michelmore RW (2003) Genome-wide analysis of NBS-LRR-encoding genes in *Arabidopsis*. Plant Cell **15:** 809–834

Monaghan J, Xu F, Gao M, Zhao Q, Palma K, Long C, Chen S, Zhang Y, Li X (2009) Two Prp19-like U-box proteins in the MOS4-associated complex play redundant roles in plant innate immunity. PLoS Pathog **5:** e1000526

Oldroyd GE, Staskawicz BJ (1998) Genetically engineered broad-spectrum disease resistance in tomato. Proc Natl Acad Sci USA **95:** 10300–10305

Palma K, Zhang Y, Li X (2005) An importin alpha homolog, MOS6, plays an important role in plant innate immunity. Curr Biol **15:** 1129–1135

Palma K, Zhao Q, Cheng YT, Bi D, Monaghan J, Cheng W, Zhang Y, Li X (2007) Regulation of plant innate immunity by three proteins in a complex conserved across the plant and animal kingdoms. Genes Dev **21:** 1484–1493

Stokes TL, Kunkel BN, Richards EJ (2002) Epigenetic variation in Arabidopsis disease resistance. Genes Dev **16:** 171–182

Swiderski MR, Birker D, Jones JD (2009) The TIR domain of TIR-NB-LRR resistance proteins is a signaling domain involved in cell death induction. Mol Plant Microbe Interact **22:** 157–165

Tian D, Traw MB, Chen JQ, Kreitman M, Bergelson J (2003) Fitness costs of R-gene-mediated resistance in Arabidopsis thaliana. Nature **423:** 74–77

Vongs A, Kakutani T, Martienssen RA, Richards EJ (1993) Arabidopsis thaliana DNA methylation mutants. Science **260:** 1926–1928

Weigel D, Ahn JH, Blazquez MA, Borevitz JO, Christensen SK, Fankhauser C, Ferrandiz C, Kardailsky I, Malancharuvil EJ, Neff MM, et al (2000) Activation tagging in Arabidopsis. Plant Physiol **122:** 1003–1013

Yi H, Richards EJ (2007) A cluster of disease resistance genes in *Arabidopsis* is coordinately regulated by transcriptional activation and RNA silencing. Plant Cell **19:** 2929–2939

Yi H, Richards EJ (2009) Gene duplication and hypermutation of the pathogen *Resistance* gene *SNC1* in the Arabidopsis *bal* variant. Genetics **183:** 1227–1234

Zhang Y, Cheng YT, Bi D, Palma K, Li X (2005) MOS2, a protein containing G-patch and KOW motifs, is essential for innate immunity in Arabidopsis thaliana. Curr Biol **15:** 1936–1942

Zhang Y, Goritschnig S, Dong X, Li X (2003a) A gain-of-function mutation in a plant disease resistance gene leads to constitutive activation of downstream signal transduction pathways in suppressor of npr1-1, constitutive 1. Plant Cell **15:** 2636–2646

Zhang Y, Li X (2005) A putative nucleoporin 96 is required for both basal defense and constitutive resistance responses mediated by suppressor of npr1-1,constitutive 1. Plant Cell **17:** 1306–1316

Zhang Y, Tessaro MJ, Lassner M, Li X (2003b) Knockout analysis of *Arabidopsis* transcription factors TGA2, TGA5, and TGA6 reveals their redundant and essential roles in systemic acquired resistance. Plant Cell **15:** 2647–2653